Robust High-Performance Bi-Directional Phase Synchronization Algorithm for Distributed and Collaborative Beamforming

Hou-Yu Zhai, Shaoshi Yang, *Senior Member, IEEE*, Xiao-Yang Wang, Jing-Sheng Tan, Yu-Song Luo, and Sheng Chen, *Life Fellow, IEEE*

***Abstract*—The distributed and collaborative beamforming (DCBF) technology has emerged as a promising enabler, which bears the potential for substantially improving both energy efficiency and communication range of low-power wireless networks, such as wireless sensor networks, millimeter-wave/terahertz communication networks, machine-to-machine communication networks, and UAV communication networks. However, since the distributed transmitters are naturally asynchronous, and both the transmitters and receivers are movable, achieving phase synchronization at the target receiver remains a critical challenge for practical implementations of DCBF. As a remedy, in this paper we propose a high-performance robust bi-directional phase synchronization algorithm for DCBF. Different from the previous works that primarily focus on optimizing adaptive phase perturbation sizes, the proposed algorithm further introduces a novel adaptive mechanism to leverage the directional information of the phase perturbation to jointly accelerate the convergence speed and improve the synchronization accuracy. Extensive simulation results are provided to validate the superior performance of the proposed phase synchronization scheme over existing state-of-the-art schemes.**

***Index Terms*—Distributed beamforming, collaborative beamforming, one-bit feedback information, feedback communication.**

I. Introduction

DISTRIBUTED and collaborative beamforming (DCBF) is widely regarded as a promising technology for enhancing transmission efficiency and extending the network lifetime in low-power wireless networks [1], such as wireless sensor networks [1], millimeter-wave/terahertz communication networks [2], and UAV communication networks [3]. The core principle of DCBF involves spatially separated transmitters cooperating with each other to form a virtual antenna array, thereby enabling collaborative signal transmission to the distant receiver [4]. However, the practical implementation of DCBF faces significant challenges, particularly in synchronizing the inherently asynchronous distributed transmitters. Specifically, the time, frequency, and phase offsets among individual distributed transmitters can severely degrade beamforming performance [4], [5]. Therefore, performing effective synchronization to compensate for these offsets is critical to guarantee coherent reception at the target destination.

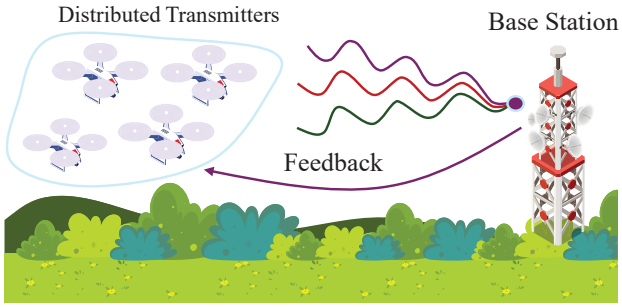

Fig. 1. Illustration of the closed-loop DCBF paradigm. Distributed transmitters collaboratively send a common signal to the target receiver, which receives and then feeds back bit-level information to all distributed transmitters.

Existing research on DCBF synchronization predominantly focuses on phase synchronization [5], which is broadly divided into two categories: open-loop and closed-loop schemes. Open-loop approaches achieve phase synchronization through direct inter-transmitter coordination [6], [7]. However, the substantial coordination overhead involved severely limits their scalability in practical deployments. In contrast, the closed-loop paradigm provides a more scalable and robust alternative. As illustrated in Fig. 1, the phases of all distributed transmitters are iteratively adjusted based on a bit-level feedback signal broadcast from the receiver, enabling large-scale, scalable synchronization with negligible coordination overhead [8]–[10]. Moreover, closed-loop schemes achieve superior phase synchronization performance by compensating for two primary sources of phase offsets: 1) the inherent phase mismatches introduced by the local oscillator of each transmitter, and 2) the channel responses between the transmitters and the receiver. Given these clear advantages, this paper focuses on the more advanced closed-loop phase synchronization framework.

Accelerating convergence speed is critical for closed-loop phase synchronization schemes, as a prolonged convergence process may fail to track channel variations in dynamic environments and escalate energy consumption. The original one-bit feedback synchronization algorithm proposed in [8] operates through iterative phase adjustments: each transmitter applies a random phase perturbation to its phase per timeslot,

This work was supported in part by Beijing Municipal Natural Science Foundation under Grant L242013, and in part by National Natural Science Foundation under Grant 62550173. *(Corresponding author: Shaoshi Yang)*

H.-Y. Zhai, S. Yang, J.-S. Tan and Y.-S. Luo are with the School of Information and Communication Engineering, Beijing University of Posts and Telecommunications, and the Key Laboratory of Mathematics and Information Networks, Ministry of Education, Beijing 100876, China (e-mails: {2hy, shaoshi.yang, jingsheng.tan, yusong.luo}@bupt.edu.cn).

X.-Y. Wang is with the Department of Wireless and Terminal Technology, China Mobile Research Institute, Beijing 100053, China (e-mail: wangxiaoyangyjy@chinamobile.com).

S. Chen is with School of Electronics and Computer Science, University of Southampton, Southampton SO17 1BJ, UK (e-mail: sqc@ecs.soton.ac.uk).

retaining it only if the target receiver returns one-bit feedback information confirming an increase in received signal strength (RSS). This simple mechanism, however, suffers from slow convergence and performance stability. To address these limitations, the work in [9] introduced dynamic perturbation-size adaptation and leveraged the single-timeslot negative feedback information to accelerate convergence speed. Building on this work, the authors of [10] further incorporated the cumulative positive feedback information to enhance steady-state performance. However, both approaches remain sensitive to the stochastic direction of the phase perturbations. Another approach in [11] utilized two consecutive feedback bits to speed up convergence, but this required tight synchronization and was sensitive to latency. The state-of-the-art (SOTA) trial-and-error (TE) learning-based phase synchronization algorithm [12] introduced state-driven adaptive perturbation size adjustment, which achieves faster convergence but at the cost of high online computational overhead.

To overcome the drawbacks of the existing solutions conceived for the above-mentioned challenges, in this paper we propose a robust, high-performance bi-directional phase synchronization algorithm for DCBF. Unlike previous approaches that focused solely on adapting the magnitude of phase perturbations, the proposed algorithm introduces a novel bi-directional adaptation mechanism. This key innovation leverages the directional information of the phase perturbations to significantly accelerate convergence, improve synchronization accuracy, and enhance system robustness. Finally, extensive simulation results are provided to validate the superior performance of our proposed method over existing schemes.

II. System Model and Original Algorithm

In this section, we begin by establishing the system model and formally defining the phase synchronization challenge for DCBF. Then, we briefly review the classic one-bit feedback phase synchronization framework in [8], highlighting its core principles and main procedure.

A. System Model Characterization

We consider a random array composed of N frequency-synchronized distributed transmitters, which collaboratively transmit a common message signal to a distant target receiver. At the target receiver, the received baseband signal at the nth timeslot is the superposition of signals from all distributed transmitters, expressed as:

$$y[n] = \sum_{i=1}^{N} \sqrt{P_i} h_i[n] e^{j\Phi_i[n]} x[n] + \omega[n], \tag{1}$$

where $x[n] \in \mathbb{C}$ is the unit-energy message signal identical across all distributed transmitters, $P_i \in \mathbb{R}$ denotes the transmitting power of the ith transmitter, $h_i[n]$ represents the channel gain from the ith transmitter to the target receiver, and $\omega[n] \sim \mathcal{CN}(0, \sigma_n^2)$ is the additive white Gaussian noise (AWGN). The term $\Phi_i[n] \in [0,\, 2\pi]$ represents the phase offset of the signal from the ith transmitter. These phase offsets, $\{\Phi_i[n]\}_{i=1}^N$, are assumed to be independently and identically distributed (i.i.d.) across distributed transmitters.

For clarity, we assume using unit transmitting power and unit channel gain in this paper, i.e., $\{P_i = 1\}_{i=1}^N$ and $\{h_i = 1\}_{i=1}^N$. Thus at the nth timeslot, the RSS at the target receiver can be simplified as

$$\text{RSS}[n] = \left| \sum_{i=1}^{N} e^{j\Phi_i[n]} + \omega[n] \right|, \tag{2}$$

and the signal-to-noise ratio (SNR) can then be defined as

$$\text{SNR}[n] = \frac{\left| \sum_{n=1}^{N} e^{j\Phi_i[n]} \right|^2}{\sigma_n^2}. \tag{3}$$

If the whole phase offsets $\{\Phi_i[n]\}_{i=1}^N$ are uncoordinated and randomly distributed, the summation $\sum_{i=1}^N e^{j\Phi_i[n]}$ *resembles a two-dimensional random walk*, which severely undermines the benefits of collaborative transmission in DCBF systems. Conversely, the maximum possible RSS is achieved when all signals arrive in perfect phase alignment, i.e., $\Phi_i[n] = constant$ for $\forall i, \forall n$. This constructive interference results in an RSS that scales linearly with the number of transmitters: $\text{RSS}_{\text{max}}[n] \propto \left| \sum_{i=1}^{N} e^{j\Phi_i[n]} \right| = N$.

In the closed-loop phase synchronization schemes, this phase alignment is achieved by having each transmitter independently and iteratively adjust its phase to compensate for a composite phase offset. To formalize this process, the total phase offset $\{\Phi_i[n]\}_{i=1}^N$ in (1) is first decomposed into the distinct physical sources. Specifically, at the nth timeslot, $\{\Phi_i[n]\}_{i=1}^N$ can be expressed as:

$$\Phi_i[n] = \gamma_i + \psi_i + \phi_i[n] + \theta_i[n],\ i \in \{1, \cdots, N\}, \tag{4}$$

where the unknown static offsets are explicitly separated into the following distinct sources:

1) $\gamma_i \in [-\pi,\, \pi]$ denotes the unknown, static phase offset inherent to the ith transmitter itself, primarily caused by hardware imperfections like local oscillator (LO) phase drift.
2) $\psi_i \in [-\pi,\, \pi]$ represents the unknown phase offset introduced by the wireless propagation channel, assumed to be static for the duration of the synchronization process.
3) $\phi_i[n] \in [-\pi,\, \pi]$ is the adaptive phase component that each transmitter actively adjusts at every timeslot, with an initialization given by $\{\phi_i[1] = 0\}_{i=1}^N$.
4) $\theta_i[n] \sim \mathcal{N}(0, \sigma_\theta^2)$ is the phase noise.

The transmitter-side offsets $\{\gamma_i\}_{i=1}^N$ are assumed to be static, uniformly distributed within $[-\pi,\, \pi]$.

Given this decomposition, the challenge of phase synchronization becomes clear. For the ith transmitter, the terms γ_i, ψ_i, and $\theta_i[n]$ are all unknown and uncontrollable. The adaptive phase component, $\phi_i[n]$, is the **sole parameter** that can be manipulated to achieve coherent combining.

Thus, the phase synchronization problem transforms into a distributed optimization task: each transmitter must intelligently and iteratively adjust its local $\{\phi_i[n]\}_{i=1}^N$ based on limited feedback, in order to compensate for the unknown aggregate phase offset $(\gamma_i + \psi_i + \theta_i[n])$ and drive the total phases of all transmitters towards a common value, thereby maximizing the RSS.

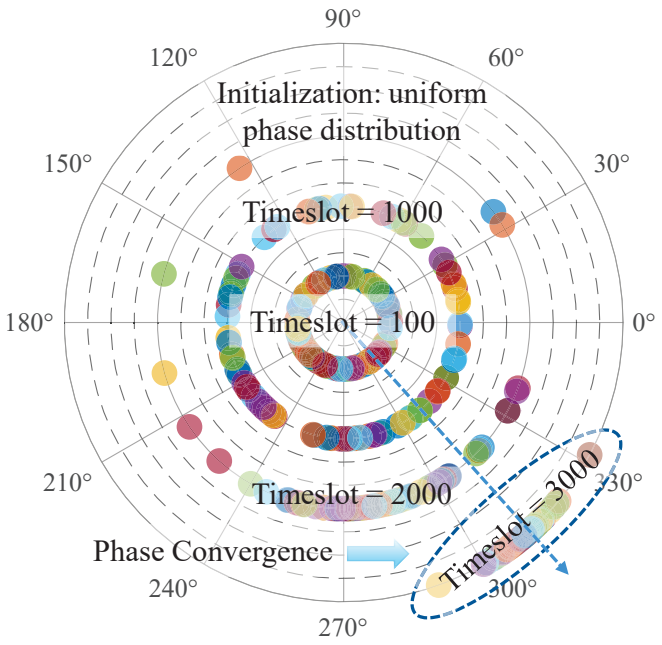

Fig. 2. Illustration of the phase convergence trace $\{\Phi_i[n]\}_{i=1}^N$ in the typical one-bit feedback beamforming algorithm with $N=50$ and $\Delta_0=\pi/10$. Here, $\{\Phi_i[n]\}_{i=1}^N$ is sampled and visualized in $n=100, 1000, 2000, 3000$.

B. Typical One-Bit Feedback Beamforming Algorithm

To maximize the RSS, the original one-bit feedback beamforming algorithm presented in [8] employs a simple yet effective iterative search mechanism. This synchronization process, which guides all distributed transmitters to achieve phase alignment, repeats the following core steps:

- **Generate Trial Phase:** At the nth timeslot, all N transmitters record their known best phases $\{\phi_i[n]\}_{i=1}^N$ and add random phase perturbations $\{\delta_i[n]\}_{i=1}^N$ to $\{\phi_i[n]\}_{i=1}^N$, where $\delta_i[n]$ is confined to the interval $[-\Delta_0, \Delta_0]$ and exhibits the probability density function $g(\delta_i)$, with $\Delta_0 > 0$ denoting the perturbation size.
- **Perform Beamforming:** All the transmitters apply the updated phase components $\{\phi_i[n]=\phi_i[n]+\delta_i[n]\}_{i=1}^N$ to attend beamforming.
- **Measure and Feedback:** The target receiver measures the current RSS, denoted as $\text{RSS}[n]$, and then updates the best RSS as:

$$\text{RSS}_{\text{best}}[n+1] = \max\{\text{RSS}_{\text{best}}[n], \text{RSS}[n]\}, \quad (5)$$

  where $\text{RSS}_{\text{best}}[n]$ is the best RSS recorded up to the$(n-1)$th timeslot. Subsequently, the target receiver broadcasts a one-bit feedback signal $\{0, 1\}$ to all transmitters to indicate whether the RSS has been improved or not.
- **Update Phase:** Based on the feedback, each transmitter updates its best-known phase for the next timeslot, $\phi_i[n+1]$. It either adopts the trial phase upon success or reverts to its previous best phase upon failure:

$$\phi_i[n+1]=\begin{cases}\phi_i[n]+\delta_i[n], & \text{RSS}[n] > \text{RSS}_{\text{best}}[n],\\ \phi_i[n], & \text{otherwise.}\end{cases} \quad (6)$$

In Fig. 2, we visualize the gradual phase alignment process. By applying the central limit theorem, the authors of [5] demonstrate that the RSS primarily depends on the cosines of the carrier phases and the contribution of the sines can be discarded for large N. Then for $i = 1,\cdots, N$, the phase updating rule in (6) of the original one-bit feedback phase synchronization algorithm can be rewritten as[1]:

$$\phi_i[n+1] = \phi_i[n] + \delta_i[n]\cdot \mathbb{1}_{\left(\sum_{i=1}^N \cos(\Phi_i[n]+\delta_i[n]) > \sum_{i=1}^N \cos(\Phi_i[n])\right)}, \quad (7)$$

where $\mathbb{1}_{\text{A}} \in \{0, 1\}$ denotes the binary indicator taking on value one if condition A holds, and zero otherwise. For a small Δ_0, a first-order Taylor series approximation yields:

$$\sum_{i=1}^N \cos(\Phi_i[n]+\delta_i[n]) \approx \sum_{i=1}^N \cos(\Phi_i[n]) - \delta_i[n]\sin(\Phi_i[n]). \quad (8)$$

Then, the phase updating rule (7) becomes:

$$\phi_i[n+1] = \phi_i[n] + \delta_i[n]\cdot \mathbb{1}_{\left(\sum_{i=1}^N \delta_i[n]\sin(\Phi_i[n]) < 0\right)}. \quad (9)$$

As proven in [8], when initialized with a random phase configuration $\{\Phi_i[0]\}_{i=1}^N$, the original one-bit feedback phase synchronization algorithm is guaranteed to converge to perfect coherent reception *almost certainly*. However, owing to its over-simplified mechanism, the original algorithm suffers from suboptimal convergence rates and stability.

III. Proposed Bi-Directional Algorithm

In this section, we propose a robust, high-performance bi-directional phase synchronization algorithm that requires no extra coordination or hardware changes compared to existing schemes. Our work is motivated by a key limitation in current one-bit feedback algorithms: while they effectively adapt the perturbation *size*, they neglect the perturbation *direction*.

Existing phase synchronization algorithms primarily focus on a one-dimensional optimization, adjusting the magnitude of the perturbation $\{\delta_i[n]\}_{i=1}^N$ based on convergence conditions, e.g., reducing the perturbation size Δ_0 to perform more precise phase adjustments when $\text{RSS}[n]/N \to 1$. However, by relying on a purely random search direction, these algorithms underutilize the feedback information and do not optimize the directional components of perturbations to achieve further improvement.

Let $\mathbf{d}[n] \triangleq [d_1[n], \ldots, d_N[n]]^{\text{T}} \in \mathbb{R}^N$, with $d_i[n] \sim \mathbb{U}[-1, 1]$ denoting the stochastic perturbation direction generated in the ith transmitter at the nth timeslot. The phase updating rule of the existing algorithms can then be expressed by

$$\mathbf{\Phi}[n+1] = \mathbf{\Phi}[n] + \mathbf{\Delta}[n]\mathbf{d}[n]\cdot \mathbb{1}_{(\text{RSS}(\mathbf{\Phi}[n]+\mathbf{\Theta}[n]) > \text{RSS}(\mathbf{\Phi}[n]))}, \quad (10)$$

where $\mathbf{\Phi}[n] = [\phi_1[n], \ldots, \phi_N[n]]^{\text{T}} \in \mathbb{R}^N$ and $\mathbf{\Delta}[n] = \Delta[n]\mathbf{I}_N \in \mathbb{R}^{N\times N}$. According to [8], the probability of a successful phase update $\mathbb{P}(\text{RSS}(\mathbf{\Phi}[n]+\mathbf{\Delta}[n]\mathbf{d}[n]) > \text{RSS}(\mathbf{\Phi}[n]))$ is significantly limited to the stochastic direction $\mathbf{d}[n]$ generated per timeslot, leading to high convergence volatility [13]. *Indeed, the convergence relies on the fortuitous alignment of the stochastic perturbation with the true gradient.*

[1]For brevity, we omit the phase noise $\{\theta_i\}_{i=1}^N$ here.

Algorithm 1 Bi-Directional Phase Synchronization Algorithm

Input: $T_{\max}$, Δ_0, Δ_{H}, Δ_{L}, α, β, C_{T1}, C_{T2}, $\mathrm{RSS}_{\mathrm{best}}$;
Initialize: Perturbation size $\Delta \leftarrow \Delta_0$, reverse perturbation buffer $\boldsymbol{\Delta}_{\mathrm{next}} \leftarrow \emptyset$, reverse flag $need\_reversed \leftarrow$ False;

for $t = 1$ **to** $T_{\max}$ **do**
  if $\boldsymbol{\Delta}_{\mathrm{next}} \neq \emptyset$ **then**
    Apply buffer perturbation: $\boldsymbol{\Delta}_{\mathrm{next}}$, clear $\boldsymbol{\Delta}_{\mathrm{next}} \leftarrow \emptyset$;
    Set reverse flag: $need\_reversed \leftarrow$ True;
  else
    Generate random perturbation: $\boldsymbol{\Delta}[n]\mathbf{d}[n]$;
    Set reverse flag: $need\_reversed \leftarrow$ False;
  end if
  Each transmitter applies trial phase to attend beamforming: $\Phi_{i,\mathrm{trial}}[n] \leftarrow \Phi_i[n] + \delta_i[n]$ for $i = 1, \ldots, N$;
  Measure current RSS: $\mathrm{RSS}[n] \leftarrow \left|\sum_{i=1}^{N} e^{j(\theta_i[n] + \Phi_{i,\mathrm{trial}}[n])}\right|$;
  if $\mathrm{RSS}[n] > \mathrm{RSS}_{\mathrm{best}}$ **then**
    $\{\Phi_i[n+1]\}_{i=1}^{N} \leftarrow \{\Phi_{i,\mathrm{trial}}[n]\}_{i=1}^{N}$, $\mathrm{RSS}_{\mathrm{best}} \leftarrow \mathrm{RSS}[n]$;
    Update success counter: $C_p \leftarrow C_p + 1$, reset $C_n \leftarrow 0$;
    if $C_p \geq C_{\mathrm{T1}}$ **then**
      Update $\Delta \leftarrow \min\{\alpha\Delta, \Delta_{\mathrm{H}}\}$, reset counter $C_p \leftarrow 0$;
    end if
  else
    if $need\_reversed =$ False **then**
      Buffer reverse perturbation: $\boldsymbol{\Delta}_{\mathrm{next}} \leftarrow -\boldsymbol{\Delta}[n]\mathbf{d}[n]$;
    else
      Clear buffer after reverse failure: $\boldsymbol{\Delta}_{\mathrm{next}} \leftarrow \emptyset$;
    end if
    Update failure counter: $C_n \leftarrow C_n + 1$, reset $C_p \leftarrow 0$;
    if $C_n \geq C_{\mathrm{T2}}$ **then**
      Update $\Delta \leftarrow \max\{\beta\Delta, \Delta_{\mathrm{L}}\}$, reset counter: $C_n \leftarrow 0$.
    end if
  end if
end for

One intuition that exploits the directional information of the random phase perturbation to achieve improvement is that: if a small phase perturbation $\boldsymbol{\Delta}[n]\mathbf{d}[n]$ lowers the current RSS, then most likely subtracting that small perturbation would improve convergence performance. By prioritizing this opposite direction in the subsequent timeslot, we transform a failed random trial into an informed and heuristic search step. This bi-directional mechanism is designed to significantly accelerate convergence. Thus, we propose the bi-directional phase synchronization algorithm as follows.

1) At the nth timeslot, the ith $(i = 1, \ldots, N)$ transmitter adjusts its best recorded phase by applying the phase perturbation $\delta_i[n]$, which is generated by $\delta_i[n] = \Delta[n]d_i[n]$.
2) All the transmitter use their adjusted trial phases $\{\phi_i[n] = \phi_i[n] + \delta_i[n]\}_{i=1}^{N}$ to attend beamforming.
3) The receiver measures $\mathrm{RSS}[n]$ and estimates whether the random phase perturbation $\{\delta_i[n]\}_{i=1}^{N}$ successfully updates the recorded best RSS, namely, $\mathrm{RSS}_{\mathrm{best}}$. If $\mathrm{RSS}_{\mathrm{best}}$ is updated, one-bit message '1' is fed back to all the transmitters; otherwise, '0' is fed back.
4) The ith transmitter receives the feedback one-bit message and updates its adaptive phase component $\phi_i[n+1]$ as:

$$\phi_i[n+1] = \begin{cases} \phi_i[n] + \delta_i[n], & \text{One-bit feedback data is 1,} \\ \phi_i[n], & \text{One-bit feedback data is 0.} \end{cases} \quad (11)$$

5) If the one-bit feedback is '0', all the transmitters update the stochastic perturbation direction as $\mathbf{d}[n+1] = -\mathbf{d}[n]$.[2]

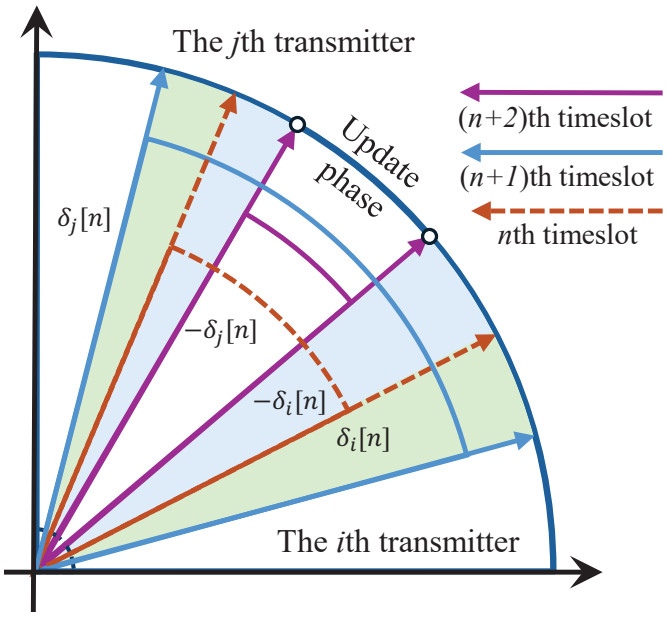

Fig. 3. Illustration of the phase update process in the proposed algorithm.

TABLE I
SIMULATION PARAMETERS AND ALGORITHM CONFIGURATION

Parameter	Value
Number of distributed transmitters	$N = 500$
Total number of timeslots	$T_{\max} = 8000$
Initial perturbation size	$\Delta[1] = 0.08\pi$
Parameter	$\alpha = 1.1$
Parameter	$\beta = 0.95$
Upper perturbation size threshold	$\Delta_{\mathrm{H}} = 0.15\pi$
Lower perturbation size threshold	$\Delta_{\mathrm{L}} = 0.01\pi$
Control parameter	$C_{\mathrm{T1}} = 4$
Control parameter	$C_{\mathrm{T2}} = 6$
Number of Monte Carlo experiments	10^3

Fig. 3 illustrates the phase update process in the proposed bi-directional algorithm. To accelerate the convergence speed, we also exploit both the cumulative positive and negative feedback information as in [10]. **Algorithm 1** summarizes the proposed bi-directional phase synchronization procedure.

IV. Numerical Results

In this section, numerical Monte Carlo simulations are performed to validate the superior performance of our proposed algorithm against several SOTA benchmarks. Specifically, the simulation study is structured as follows:

[2]In fact, there exists a situation where neither $\mathbf{d}[n]$ nor $\mathbf{d}[n+1] = -\mathbf{d}[n]$ can increase the current $\mathrm{RSS}[n]$. In this case, we regenerate the random perturbation direction $\mathbf{d}[n+1]$ at the next timeslot.

TABLE II
THE RSS CONVERGENCE ACCURACY OF DIFFERENT SCHEMES WITH DIFFERENT PHASE NOISE CONFIGURATIONS

Scheme	$\sigma_\theta^2=0.005$	$\sigma_\theta^2=0.01$	$\sigma_\theta^2=0.015$	$\sigma_\theta^2=0.02$	$\sigma_\theta^2=0.025$	$\sigma_\theta^2=0.03$	$\sigma_\theta^2=0.035$	$\sigma_\theta^2=0.04$
Original Algorithm [8]	0.9620	0.9454	0.8506	0.6937	0.4993	0.3545	0.2292	0.1723
Algorithm in [9]	0.9678	0.9419	0.8608	0.7453	0.6405	0.6066	0.4492	0.3414
Algorithm in [10]	0.9778	0.9251	0.7850	0.6228	0.4594	0.4009	0.3353	0.2641
Algorithm in [11]	0.3293	0.2150	0.1949	0.1598	0.1191	0.0948	0.0853	0.0824
Algorithm in [12]	0.9570	0.8506	0.9372	0.8809	0.7320	0.4832	0.4475	0.3293
Proposed Algorithm	**0.9720**	**0.9504**	**0.9149**	**0.8120**	**0.6868**	**0.6173**	**0.5585**	**0.5157**

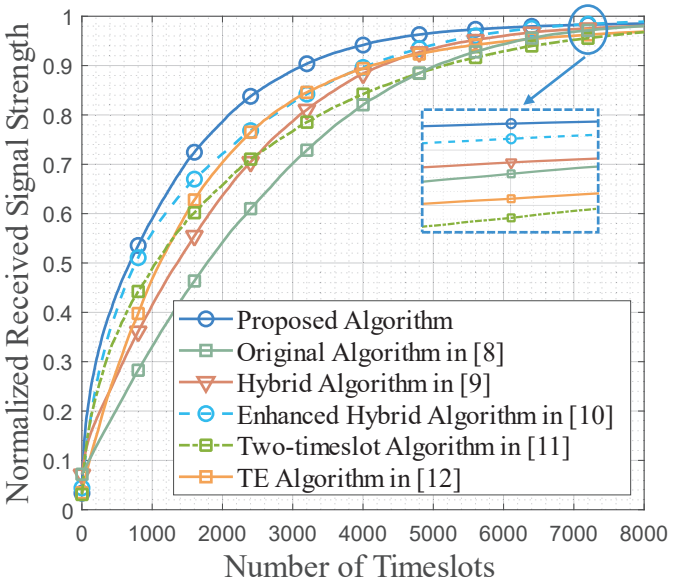

Fig. 4. Convergence speed comparison for the proposed algorithm and five existing algorithms.

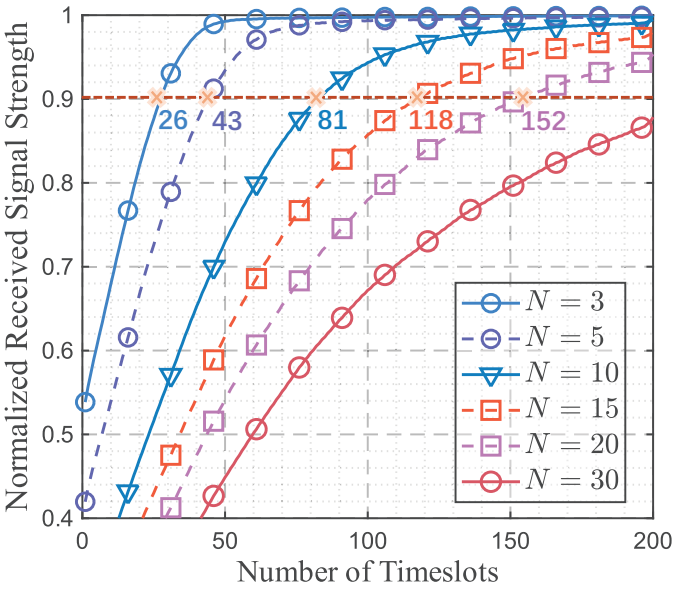

Fig. 5. Convergence performance for various network scales.

1) First, the fundamental convergence speed and synchronization accuracy are evaluated by omitting the phase noise $\{\theta_i[n]\}_{i=1}^N$ and the AWGN for simplicity;
2) Second, the robustness of the proposed algorithm against dynamic channel changes and phase noise is assessed;
3) Finally, the optimal parameter configuration for the proposed algorithm is determined.

The general simulation parameters are summarized in Table I, unless stated otherwise. In addition, we utilize the complete Jake's channel model [14] and each set of results is derived from 10^3 independent Monte Carlo experiments.

A. Convergence Performance Analysis

First, a performance baseline is established by evaluating the convergence speed and accuracy in a noise-free setting. The metric used is the normalized RSS, $\text{RSS}[n]/N$. As shown in Fig. 4, the proposed algorithm consistently exhibits the best convergence performance among all schemes. Although the enhanced hybrid algorithm [10] shows a comparable initial convergence rate, it is quickly surpassed by the proposed algorithm. This superior performance is attributed to the proposed bi-directional mechanism, which effectively converts failed trials into productive search steps, thereby minimizing wasted timeslots and accelerating the ascent towards optimal phase alignment.

To further validate the practicality of the proposed algorithm, its convergence performance is evaluated in smaller, more realistic network scales. As shown in Fig. 5, the algorithm demonstrates rapid convergence that meets real-time requirements. For instance, in a network with $N = 3$ transmitters, the algorithm reaches 90% of the optimal RSS in just 26 timeslots.

B. Robustness Evaluation

Next we evaluate the robustness of different phase synchronization algorithms. As illustrated in Fig. 6, we first consider the situation in which a sudden channel change occurs at the 3000th timeslot. The channel phases $\{\psi_i\}_{i=1}^N$ are modeled as Jake's channel, and the abrupt change is simulated by completely randomizing all channel phases $\{\psi_i\}_{i=1}^N$ at this specific timeslot. The SNR at the receiver is set to 15 dB. By comparing the results in Fig. 6, it can be seen that the proposed algorithm continues to exhibit the best performance.

Then, we evaluate the robustness of all the algorithms under different intensities of phase noise $\{\theta_i\}_{i=1}^N$. Table II compares the final convergence accuracy $\text{RSS}[T_{\max}]/N$ after $T_{\max} = 8000$ timeslots. The results demonstrate that our scheme consistently outperforms all other benchmarks. While

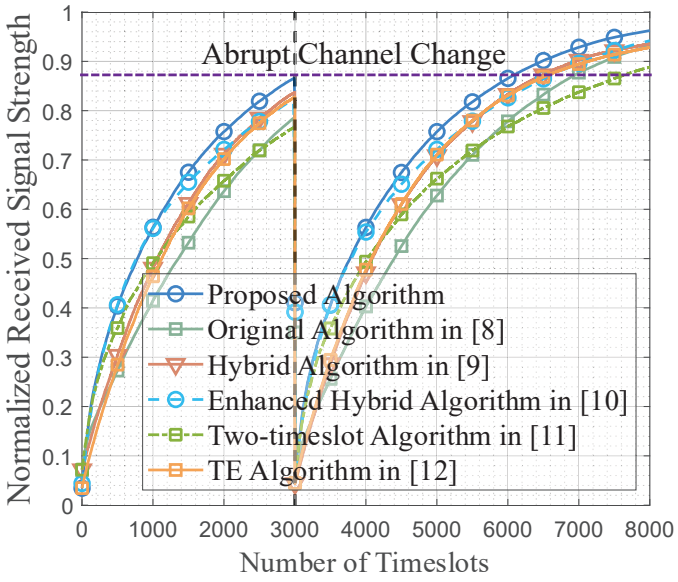

Fig. 6. Convergence speed comparison for the proposed algorithm and five existing algorithms, when the channel changed suddenly at timeslot $n = 3000$.

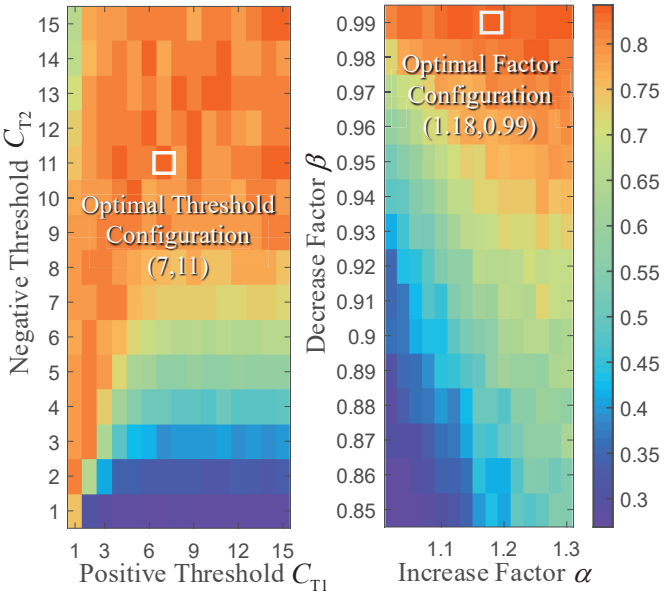

Fig. 7. The optimal parameter $\{C_{T1}, C_{T2}\}$ and $\{\alpha, \beta\}$ configuration for the proposed algorithm.

several algorithms perform well under low-noise conditions, their accuracy degrades sharply as the phase noise variance σ_θ^2 increases. In contrast, our algorithm exhibits much more graceful performance degradation. For instance, at the highest noise level $\sigma_\theta^2 = 0.04$, our algorithm achieves an accuracy of 0.5157, significantly outperforming the next-best scheme, confirming the strong noise-suppression capability.

C. Parameter Optimization

Finally, to determine the optimal parameter configuration $\{C_{T1}, C_{T2}, \alpha, \beta\}$ for our proposed phase synchronization algorithm, we evaluated the final convergence accuracy $\text{RSS}[T_{\max}]/N$ under various combinations of $\{C_{T1}, C_{T2}\}$ and $\{\alpha, \beta\}$, and the results are depicted in Fig. 7. As can be seen from the left sub-figure, the optimal $\{C_{T1}, C_{T2}\}$ configuration is given by $\{7, 11\}$. Similarly, the optimal $\{\alpha, \beta\}$ configuration is determined as $\{1.18, 0.99\}$ from the right sub-figure.

V. Conclusion

Since the distributed transmitters are naturally asynchronous, achieving phase synchronization at the target receiver remains a critical challenge for DCBF implementations. In this paper, we have presented a robust high-performance bi-directional phase synchronization algorithm for DCBF. Different from the existing works that primarily focus on adaptive perturbation size adjustment, our proposed algorithm has further introduced bi-directional adaptation of random phase perturbations to accelerate the convergence rate as well as enhance convergence accuracy. Extensive simulation results have validated the superior performance of the proposed algorithm over existing SOTA benchmark phase synchronization schemes.

References

[1] S. Jayaprakasam, S. K. Abdul Rahim, and C. Y. Leow, "Distributed and collaborative beamforming in wireless sensor networks: Classifications, trends, and research directions," *IEEE Communi. Surveys & Tutorials*, vol. 19, no. 4, pp. 2092–2116, Fourthquarter 2017.

[2] Z. Xiao, *et al.*, "A survey on millimeter-wave beamforming enabled UAV communications and networking," *IEEE Communi. Surveys & Tutorials*, vol. 24, no. 1, pp. 557–610, Firstquarter 2022.

[3] S. Liang, *et al.*, "Cooperative communication via automated guided vehicle and unmanned aerial vehicle: A distributed collaborate beamforming method," *IEEE Trans. Intelligent Vehicles*, vol. 10, no. 5, pp. 3368–3381, May 2025.

[4] X. Zheng, *et al.*, "Reliable and energy-efficient communications via collaborative beamforming for UAV networks," *IEEE Trans. Wireless Communi.*, vol. 23, no. 10, pp. 13235–13251, Oct. 2024.

[5] S. Hanna and D. Cabric, "Distributed transmit beamforming: Design and demonstration from the lab to UAVs," *IEEE Trans. Wireless Communi.*, vol. 22, no. 2, pp. 778-792, Feb. 2023.

[6] T. P. Bidigare, *et al.*, "Wideband distributed transmit beamforming using channel reciprocity and relative calibration," in *Proc. ACSSC 2015* (Pacific Grove, CA, USA), Nov. 8-11, 2015, pp. 271–275.

[7] E. Vlachos and K. Berberidis, "Blind distributed beamforming via matrix completion," in *Proc. SPAWC 2016* (Edinburgh, UK), Jul. 3-6, 2016, pp. 1–6.

[8] R. Mudumbai, J. Hespanha, U. Madhow, and G. Barriac, "Distributed transmit beamforming using feedback control," *IEEE Trans. Information Theory*, vol. 56, no. 1, pp. 411–426, Jan. 2010.

[9] S. Song, J. S. Thompson, P.-J. Chung, and P. M. Grant, "Exploiting negative feedback information for one-bit feedback beamforming algorithm," *IEEE Trans. Wireless Communi.*, vol. 11, no. 2, pp. 516–525, Feb. 2012.

[10] N. Xie, K. Xu, and J. Chen, "Exploiting cumulative positive feedback information for one-bit feedback synchronization algorithm," *IEEE Trans. Vehicular Technology*, vol. 67, no. 7, pp. 5821–5830, Jul. 2018.

[11] H. Yang, *et al.*, "A novel one-bit feedback collaborative beamforming algorithm using two time slots," in *Proc. ICCC 2017* (Chengdu, China), Dec. 13-16, 2017, pp. 857–861.

[12] M. Iqbal, *et al.*, "Distributed beamforming using trial and error learning algorithm," in *Proc. APCC 2021* (Kuala Lumpur, Malaysia), Oct. 11-13, 2021, pp. 275–280.

[13] X. Yi, *et al.*, "ArguteDUB: Deep learning based distributed uplink beamforming in 6G-based IoV," *IEEE Trans. Mobile Computing*, vol. 23, no. 4, pp. 2551–2565, Apr. 2024.

[14] Y. R. Zheng and C. Xiao, "Simulation models with correct statistical properties for Rayleigh fading channels," *IEEE Trans. Communi.*, vol. 51, no. 6, pp. 920–928, Jun. 2003